Supplemental data

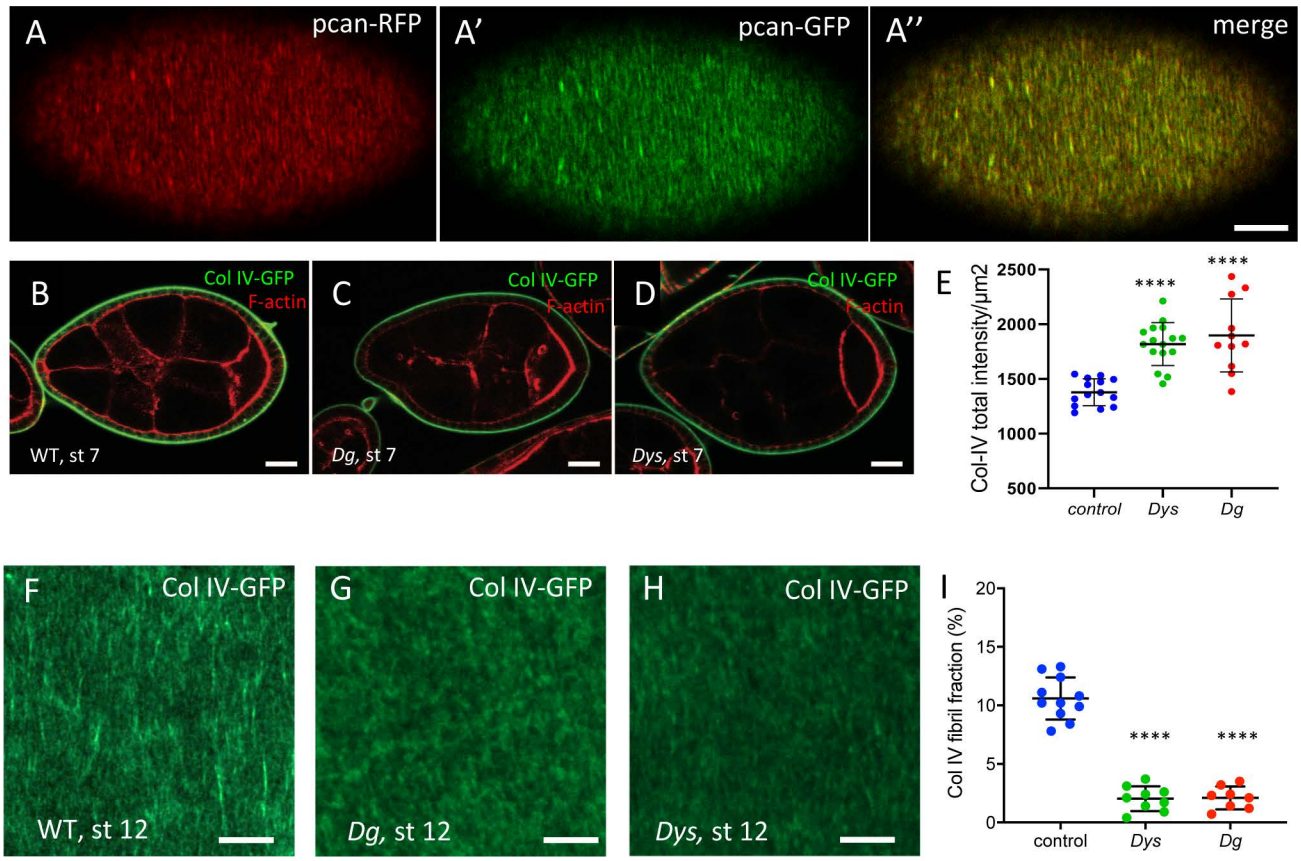

Figure S1

A) Basal view of the ECM of stage 7 from fly trans-heterozygous flies for *Pcan-RFP* and *Pcan-GFP*

B-D) Optical cross-section of stage 7 WT, $Dys^{E17/Exel6184}$ and $Dg^{O46/O83}$mutant follicles that express ColIV-GFP and stained for F-actin.

E) Quantification of the total fluorescence intensity per area unit in stage 8 WT, $Dys^{E17/Exel6184}$ and $Dg^{O46/O83}$ null mutant follicles.

F-H) Basal view of the ECM of stage 12 WT, $Dys^{E17/Exel6184}$ and $Dg^{O46/O83}$ null mutant follicles that express ColIV-GFP.

I) Quantification of the BM fibril fraction in stage 12 WT, $Dys^{E17/Exel6184}$ and $Dg^{O46/O83}$ null mutant follicles. Scalebar 10µm.

For all panels error bars represent s.d.; p *< 0.01, **<0.005, ***<0.001, ****<0.0001.

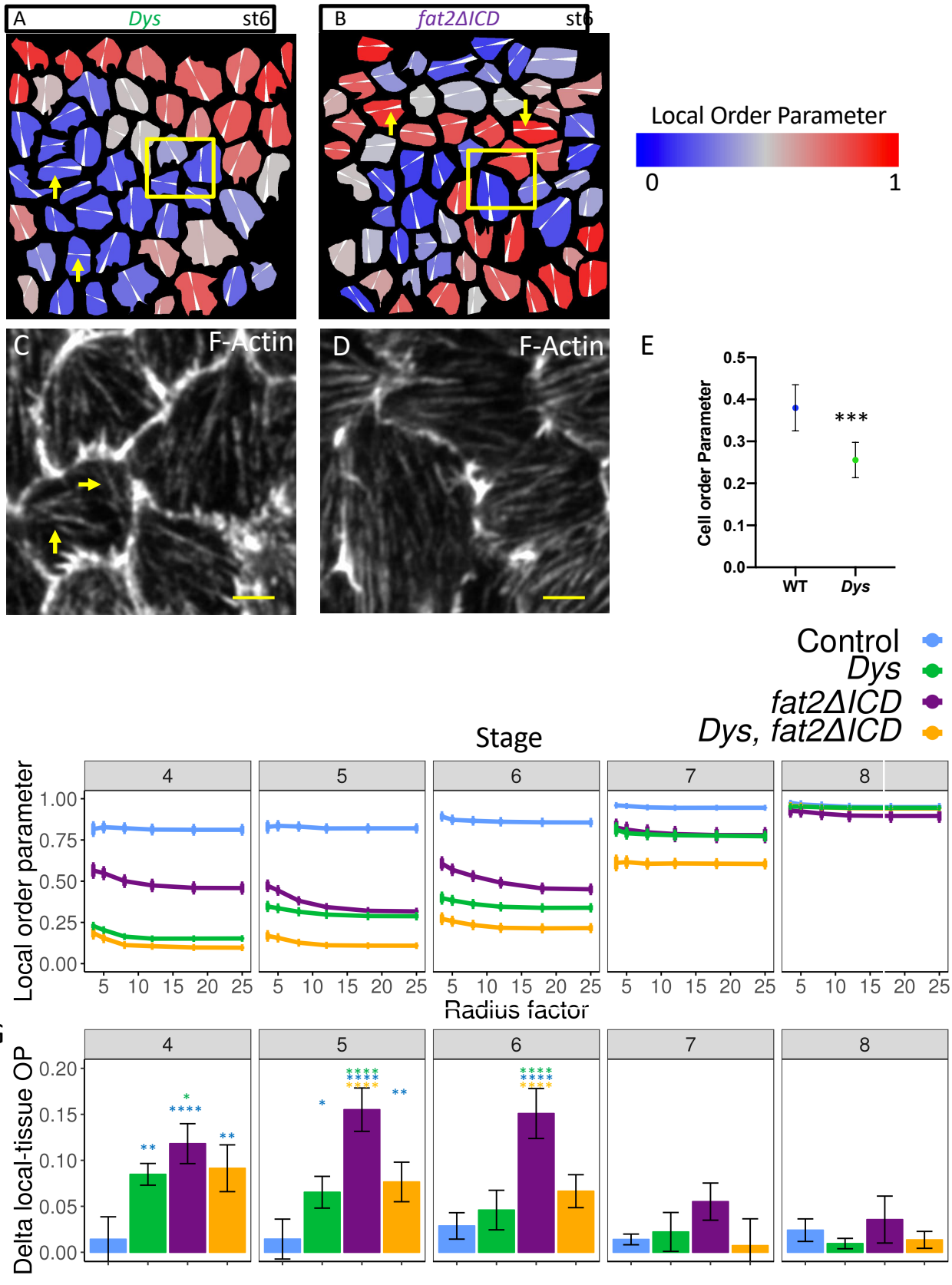

Figure S2:

A-B) Color coding of the Local OP by cell on representative images (B and C of Fig. 4) of A) *Dys*$^{E17/Exel6184}$ and B) f*at2deltaICD* mutants. Main orientation of the stress fibers is indicated in white. Note that cells with a wrong orientation (yellow arrows) can have a high Local OP in *fat2deltaICD* mutant (but not in *Dys* mutant) indicating that they are surrounded by cells with a similar orientation. C-D) Zoom-in corresponding to the yellow squares in A and B. Yellow arrows highlight divergent stress fibers in a same cell in *Dys* mutant.

E) Cell Order Parameter for *Dys* mutant cells and WT neighboring cells at stage 5 (n >138 cells).

F) Representation for stages 4 to 8 of the Local OP as a function of the distance (measured in cell radius), showing the tendency from Local OP to Tissue OP. G) Difference between Local OP (minimal value for radius in E) and Tissue OP (maximal value for radius in E) (n > 171 cells for each stage and each genotype).

For all panels error bars represent s.d.; p *< 0.01, **<0.005, ***<0.001, ****<0.0001. Scale bar 2µm

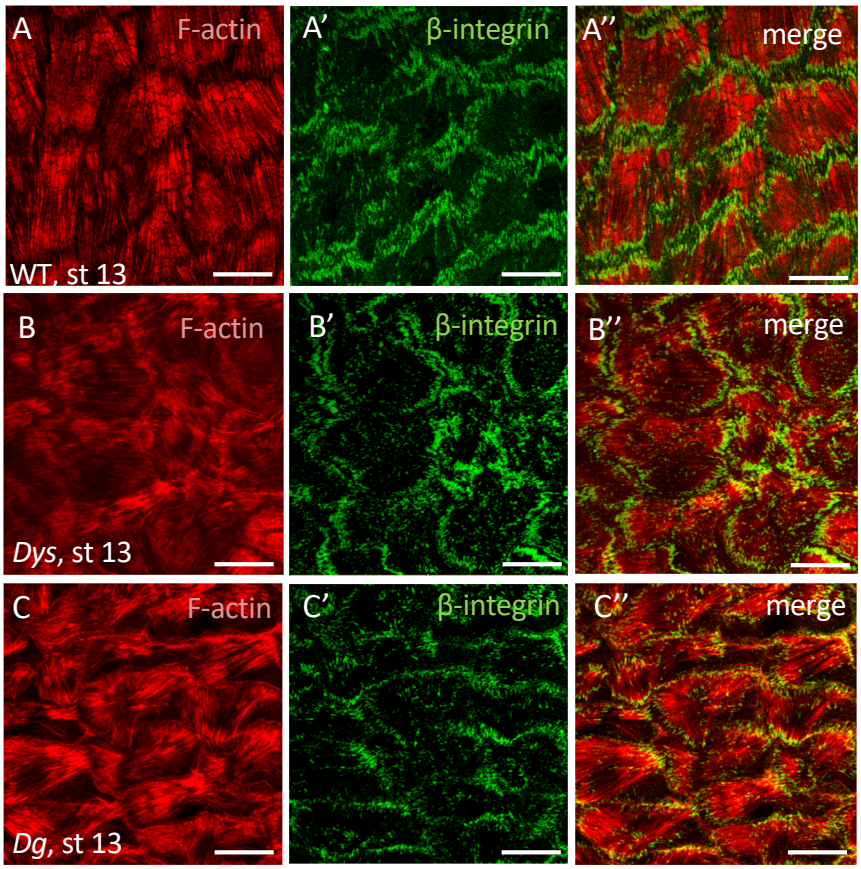

Figure S3:

F-actin and Beta-integrin staining in A) WT, B) *Dys* $^{E17/Exel6184}$ and C) *Dg* $^{O46/O83}$ mutant follicles at stage 13.

Scale bar 10µm

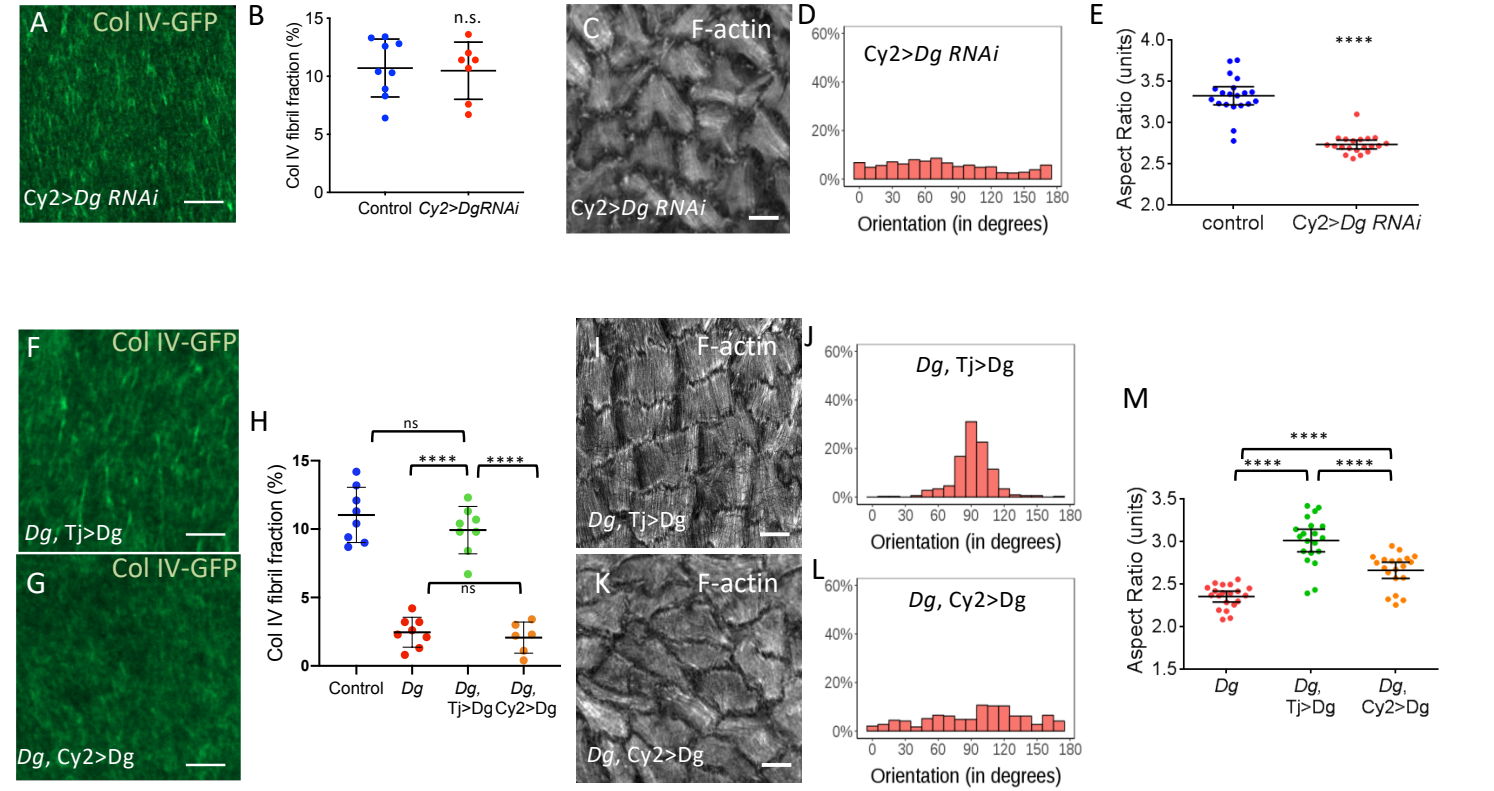

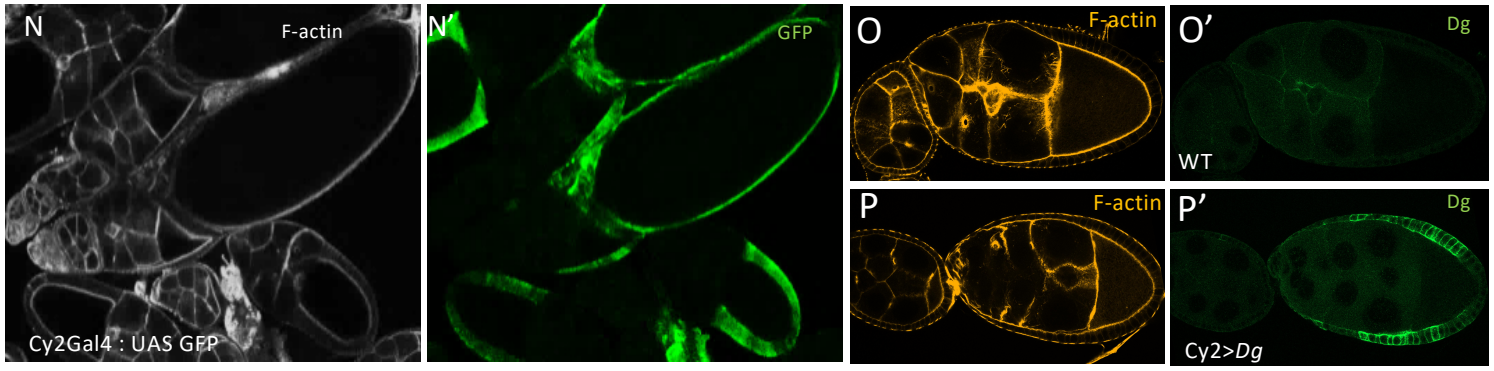

Figure S4:

A,F,G) Basal view of the ECM at stage 12 of A) Dg RNAi driven with Cy2:Gal4, F) *Dg*$^{O46/O83}$ mutant expressing UAS:Dg driven with tj:Gal4, G) Dg mutant expressing UAS:Dg driven with Cy2:Gal4

B,H) Quantification of the BM fibril fraction for the indicated genotypes at stages 12.

C,I,K) Representative images of basal F-actin at stage 13 of C) Dg RNAi driven with Cy2:Gal4, I) Dg mutant expressing UAS:Dg RNAi driven with tj:gal4, K) *Dg* mutant expressing UAS:Dg RNAi driven with Cy2:Gal4

D,J, L) Quantification of stress fiber angular distribution of the same genotypes than in C,J,K).

E, M) Aspect-Ratio quantification of mature eggs of the indicated genotypes.

N) Expression profile of Cy2:Gal4. GFP can be detected from stage 9.

O-P) Dg immunostaining in WT and Cy2:Gal4 UAS:Dg flies. Endogenous Dg is not detected but induced expression is clearly detectable at stage 9.

(For all panels error bars represent s.d.; p *< 0.01, **<0.005, ***<0.001, ****<0.0001) Scale bar 10µm.

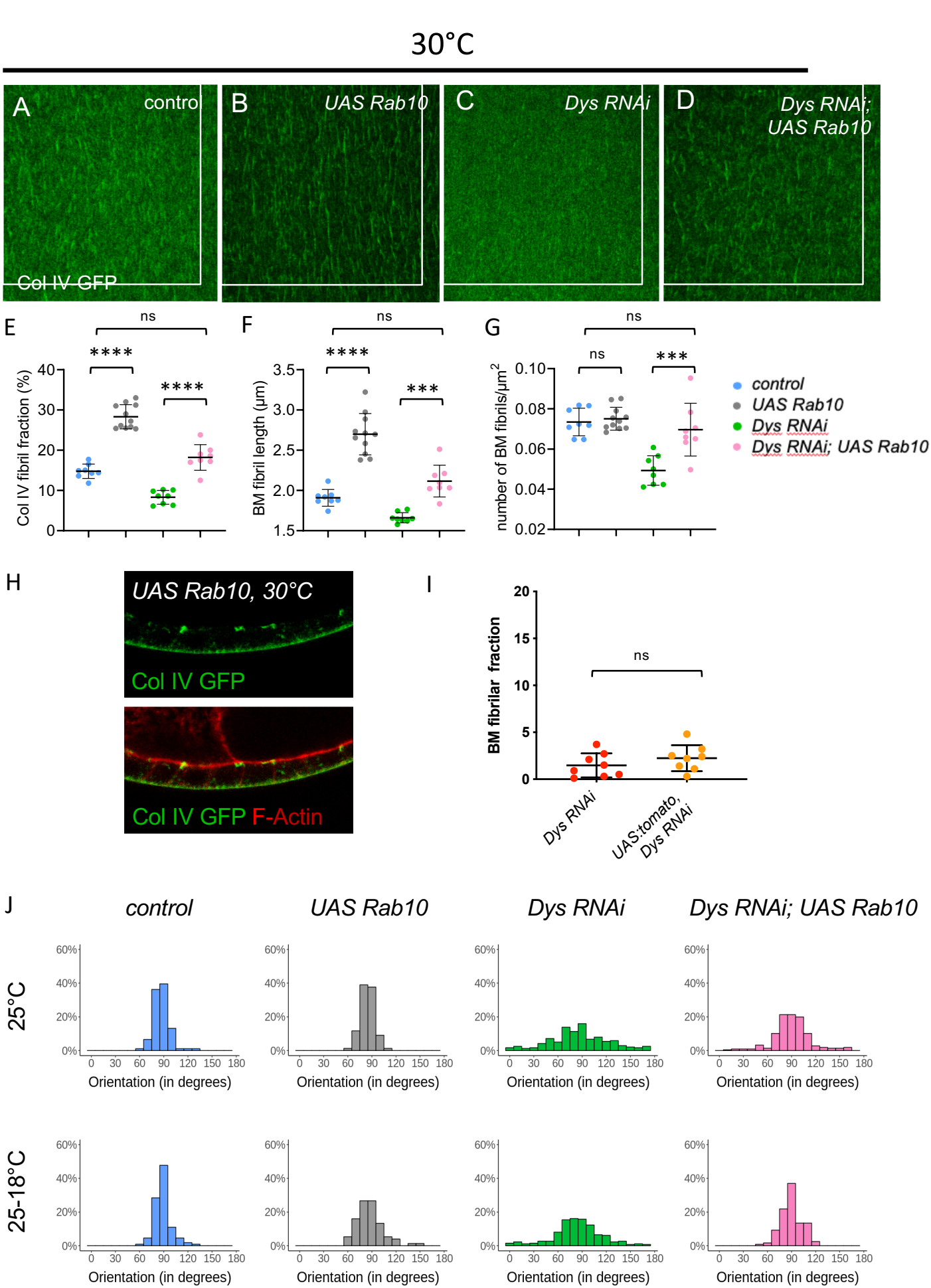

Figure S5:

A-D) Basal view of the ECM at stage 8 of A) WT, B) tj:Gal4>UAS:Rab10, C) tj:Gal>UAS Dys RNAi, D) tj:Gal4> UAS Dys RNAi, UAS Rab10.

E-G) Quantification of E) BM fibril fraction F) fibril length and G) fibril numbers per μm^2 at stage 8 for the indicated genotypes at 30°C (n>8). (error bars represent s.d.; p *< 0.01, **<0.005, ***<0.001, ****<0.0001)

H) Section view of the follicular epithelium expressing ColIV-GFP and overexpressing Rab10 at 30°C.

I) Quantification of fibril fraction at stage 12 for tj>*Dys* RNAi and tj>UAS:tomato; *Dys* RNAi

J) Angular distribution for the indicated genotypes without (25°C) or with (25-18°C) a switch to non-permissive temperature.

Table S1: Genotypes and specific conditions

Figure		Genotype	Conditions
Figure 1	B, E,F,G,H,I,L	WT (w^{1118})	
	C,E,F,GH,J, L	$Dys^{E17}/Dys^{Exel6184}$	25°C
	D,E,F,G,H,K,L	Dg^{O43}/Dg^{O86}	
	E,F,G	Dg^{O43}/Dg^{O86}; $Dys^{E17}/Dys^{Exel6184}$	
Figure 2	A	Trol-RFP/+ ; CollV-GFP/+	
	B	Trol-RFP/+ ; ; LanA-GFP/+	
	C	Trol-RFP/+ ; ; $Dys^{E17}/Dys^{Exel6184}$	
	D	CollV-GFP/+ ; $Dys^{E17}/Dys^{Exel6184}$	25°C
	E	Dys^{E17}/LanA-GFP, $Dys^{Exel6184}$	
	F, G,H	WT $Dys^{E17}/Dys^{Exel6184}$ Dg^{O43}/Dg^{O086}	
	I, J	y,w,HS:flp122/+;;FRT82B, Ubi:RFP^{nls}/FRT82B, $Dys^{Exel6184}$	25°C, 2HS 1H, dissection 5 days after HS
	K	$fat2^{N103-2}/fat2^{58D}$	25°C
	L	$fat2^{N103-2}$, $Dys^{E17}/fat2^{58D}$, $Dys^{Exel6184}$	25°C
FigureS1	A	Pcan-RFP / Pcan-GFP	
	B,E, F, I	CollV-GFP/+	
	C,G,E,I	CollV-GFP, Dg^{O86}/Dg^{O43}	25°C
	D, H,E, I	CollV-GFP/+ ; $Dys^{E17}/Dys^{Exel6184}$	
Figure 3	A-F,T	WT	
	G-L,T	$Dys^{E17}/Dys^{Exel6184}$	25°C
	M-R,T	Dg^{O43}/Dg^{O86}	
	U, V	y,w,HS:flp122/+ ;; FRT82B,Ubi:RFP^{nls} / FRT82B, $Dys^{Exel6184}$	25°C, 2HS 1H, dissection 5 days after HS
Figure 4	A,I,J,K,L,M,Q,R	WT	
	B, I,J,K,L,N,Q,R	$Dys^{E17}/Dys^{Exel6184}$	25°C
	C, I,J,K,L,O,Q,R	$fat2^{N103-2}$/ fat2DeltaICD-3xGFP	
	D, I,J,K,L,P,Q,R	$fat2^{N103-2}$, Dys^{E17}/ fat2DeltaICD-3xGFP, $Dys^{Exel6184}$	
Figure S2	F, G	WT	
	A,C, F, G	$Dys^{E17}/Dys^{Exel6184}$	25°C
	E	y,w,HS:flp122/+ ;; FRT82B,Ubi:RFP^{nls} / FRT82B, $Dys^{Exel6184}$	
	B,D,F,G	$fat2^{N103-2}$/ fat2DeltaICD-3xGFP	
	F,G	$fat2^{N103-2}$, Dys^{E17}/ fat2DeltaICD-3xGFP, $Dys^{Exel6184}$	
Figure 5	A-D	WT	
	E-H	$Dys^{E17}/Dys^{Exel6184}$	25°C
	I-L	Dg^{O86}/Dg^{O43}	
	M,N	y,w,HS:flp122/+;FRTG13, Ubi:GFP^{nls}/FRTG13, Dg	
Figure S3	A	WT	
	B	$Dys^{E17}/Dys^{Exel6184}$	25°C
	C	Dg^{O86}/Dg^{O43}	
Figure 6	B-E	Tj:Gal4, CollV-GFP; tub:Gal80^{ts}/+	18°C
		Tj:Gal4,CollV-GFP / UAS: Dg-RNAi ; tub:Gal80^{ts}/+	
	F-I	Tj:Gal4, CollV-GFP; tub:Gal80^{ts}/+	30°C
		Tj:Gal4,CollV-GFP / UAS: Dg-RNAi ; tub:Gal80^{ts}/+	

	L-O	Tj:Gal4, CollV-GFP; tub:Gal80^{ts}/+ Tj:Gal4,CollV-GFP / UAS: Dg-RNAi ; tub:Gal80^{ts}/+	18°C switch at 30°C during 30 hours
	P-S	Tj:Gal4, CollV-GFP; tub:Gal80^{ts}/+ Tj:Gal4,CollV-GFP / UAS: Dg-RNAi ; tub:Gal80^{ts}/+	30°C switch at 18°C during 72 hours
Figure S4	A-E	Cy2:Gal4, CollV-GFP/ + Cy2:Gal4, CollV-GFP/UAS Dg RNAi	Cross at 25°C ,2days at 30°C
	F,H,I,J,M	Tj:Gal4,CollV-GFP, *Dg^{O86}* / UAS: Dg-C, *Dg^{O43}*	25°C
	G,H,K,L,M	Cy2:Gal4,CollV-GFP, *Dg^{O86}* / UAS: Dg-C, *Dg^{O43}*	25°C
	H,M	CollV-GFP, *Dg^{O86}/Dg^{O43}*	25°C
	N	Cy2:Gal4/UAS-GFP	18°C
	O	WT	
	P	Cy2:Gal4 /UAS-DG	25°C
Figure 7	A	Tj:Gal4, CollV-GFP Tj:Gal4, CollV-GFP /UAS *Dys* RNAi Tj:Gal4, CollV-GFP; UAS:Rab10-RFP Tj:Gal4, CollV-GFP /UAS *D*ys RNAi ; UAS:Rab10-RFP	25°C
	B-K	Tj:Gal4; tub:Gal80^{ts} Tj:Gal4; tub:Gal80^{ts} /UAS *Dys* RNAi Tj:Gal4; tub:Gal80^{ts}; UAS:Rab10-RFP Tj:Gal4; tub:Gal80^{ts} /UAS *D*ys RNAi ; UAS:Rab10-RFP	25°C with or w/o switch at 18°C during 72 hours
Figure S5	A,E,F,G	Tj:Gal4, CollV-GFP	
	B,E,F,G,H	Tj:Gal4, CollV-GFP; UAS:Rab10-RFP	30°C
	C,E,F,G	Tj:Gal4, CollV-GFP /UAS *Dys* RNAi	
	D,E,F,G	Tj:Gal4, CollV-GFP /UAS *D*ys RNAi ; UAS:Rab10-RFP	
	I	Tj:Gal4, CollV-GFP /UAS *Dys* RNAi Tj:Gal4, CollV-GFP /UAS *D*ys RNAi ; UAS:tomato	
	J	Tj:Gal4; tub:Gal80^{ts} Tj:Gal4 ; tub:Gal80^{ts}; UAS:Rab10-RFP Tj:Gal4 ; tub:Gal80^{ts} /UAS *Dys* RNAi Tj:Gal4; tub:Gal80^{ts} /UAS *D*ys RNAi ; UAS:Rab10-RFP	25°C with or w/o switch at 18°C during 72 hours

Table S2 : RESOURCES and REAGENT TABLE

REAGENT or RESOURCE	SOURCE	IDENTIFIER
Antibodies		
Anti-GFP, goat	Abcam	5450
Laminin, Guinea Pig	(Harpaz and Volk 2012) (Volk lab)	N/A
Beta integrin, mouse	Developmental Studies Hybridoma Bank	CF.6G11
Chemicals, Peptides, and Recombinant Proteins		
FM4-64	Invitrogen	T13320
Phalloidin Alexa568 or Alexa 488	invitrogen	A12380 or A12379
Experimental Models: Organisms/Strains		
w^{1118}	Bloomington Drosophila Stock Center	FlyBase ID: FBal0018186 BDSC:3605
Dg^{O86}	{Christoforou 2008} (Rob Ray)	FlyBase ID: FBal0218114
Dg^{O43}	Christoforou 2008} (Rob Ray)	FlyBase ID: FBal0218112
Dys^{E17}	Christoforou 2008} (Rob Ray)	FlyBase ID: FBal0241311
Dys^{Exel6184}*: FRT 82B,* Df(3R)Exel6184	Bloomington Drosophila Stock Center	BDSC: 7663; FlyBase ID: FBab0038239
RNAi Dg: UAS:Dg(KK100828)	Vienna Drosophila Resource Center	FBal0230939 VDRC: v107029
RNAI Dys : UAS :Dys(KK101285)	Vienna Drosophila Resource Center	FBal0231174 VDRC: v108006
Pcan-GFP : P{PTT-un1}trol^{1973}	Kyoto Stock Center (DGRC)	FlyBase ID: FBal0191079 : DGRC : 110836
collV-GFP : P{PTT-un1}CollV^{G205}	Kyoto Stock Center (DGRC)	FlyBase ID: FBti0074199; DGRC: 110626
LanA-GFP : LanA(fTRG00574.sfGFP-TVPTBF)	Vienna Drosophila Resource Center	VDRC: v318155 FlyBase ID: FBal0339089
Pcan-mCherry	This paper	based on MI03800
UAS:Rab10-RFP	Isabella and Horne-Badovinac, 2016	
UAS: tomato	Bloomington Drosophila Stock Center	BDSC: 30124
Tj:Gal4 : P{w+mW.hs=GawB}NP1624	Kyoto Stock Center	DGRC: 104055 FlyBase ID: FBti0034540
Cy2:Gal4 : w; P{GawB}CY2	{Queenan 1997} (St Johnston lab)	FlyBase ID: FBti0007266

Tub:Gal80ts : w[*]; sna[Sco]/CyO; P{w[+mC]=tubP-GAL80[ts]}7	Bloomington Drosophila Stock Center	BDSC: 67071; FlyBase ID: FBti0027798
Fat2^{N103-2}	{HorneBadovinac 2012}	FlyBase ID: FBal0267777
Fat2^{58D}	{Viktorinová 2009} (Dhamann	FlyBase ID: FBal0241216
UAS:Dg-C	(Deng et al, 2003) (Ruhola-Baker lab)	FlyBase ID: FBal0145088
FRTG13, Ubi:GFP^{nls} : w[1118]; P{w[+mW.hs]=FRT(w[hs])}G13 P{w[+mC]=Ubi-GFP.nls}2R1 P{Ubi-GFP.nls}2R2	Bloomington Drosophila Stock Center	BDSC: 5826
Fat2-DeltaICD-3xGFP	(Barlan et al, 2017)	FlyBase ID: FBal0326665
y,w, hs:flp : P{ry[+t7.2]=hsFLP}22, w[*]	Bloomington Drosophila Stock Center	BDSC: 8862; FlyBase ID: FBst0008862
Software and Algorithms		
Fiji	(Schindelin et al, 2012)	
R		
Prism		

Table S3: Results of the statistical analysis for Fig 7I-L

test genotype 1- genotype 2	LOP p value	COP p value	TOP p value	Delta LOP -TOP p value
Stage 4:				
WT-Fat2ΔICD	<.0001	0.9990	0.0008	<.0001
WT-Dys,Fat2ΔICD	<.0001	<.0001	<.0001	0.0038
WT-Dys	<.0001	<.0001	<.0001	0.0023
Fat2ΔICD-Dys,Fat2ΔICD	<.0001	<.0001	<.0001	0.3807
Fat2ΔICD-Dys	<.0001	<.0001	0.0055	0.0452
Dys,Fat2ΔICD-Dys	0.0613	0.8408	0.4865	0.9629
Stage 5:				
WT-Fat2ΔICD	<.0001	<.0001	<.0001	<.0001
WT-Dys,Fat2ΔICD	<.0001	<.0001	<.0001	0.0059
WT-Dys	<.0001	<.0001	<.0001	0.0166
Fat2ΔICD-Dys,Fat2ΔICD	<.0001	<.0001	0.0250	<.0001
Fat2ΔICD-Dys	<.0001	<.0001	0.9973	<.0001
Dys,Fat2ΔICD-Dys	<.0001	0.3865	0.0413	0.8432
Stage 6:				
WT-Fat2ΔICD	<.0001	<.0001	0.0004	<.0001
WT-Dys,Fat2ΔICD	<.0001	<.0001	<.0001	0.1535
WT-Dys	<.0001	<.0001	<.0001	0.7643
Fat2ΔICD-Dys,Fat2ΔICD	<.0001	<.0001	0.0209	<.0001
Fat2ΔICD-Dys	<.0001	<.0001	0.8242	<.0001
Dys,Fat2ΔICD-Dys	<.0001	0.6676	0.1256	0.3830
Stage 7:				
WT-Fat2ΔICD	<.0001	0.0549	0.5779	0.2422
WT-Dys,Fat2ΔICD	<.0001	<.0001	0.0079	0.9879
WT-Dys	<.0001	<.0001	0.5052	0.9830
Fat2ΔICD-Dys,Fat2ΔICD	<.0001	<.0001	0.3924	0.0844
Fat2ΔICD-Dys	0.9693	<.0001	1.0000	0.4280
Dys,Fat2ΔICD-Dys	<.0001	0.5118	0.4610	0.8844
Stage 8:				
WT-Fat2ΔICD	0.4559	0.0574	0.9600	0.9742
WT-Dys,Fat2ΔICD	0.9388	0.5843	1.0000	0.9784
WT-Dys	0.9164	0.9753	1.0000	0.9538
Fat2ΔICD-Dys,Fat2ΔICD	0.7539	0.4490	0.9685	0.8093
Fat2ΔICD-Dys	0.8422	0.0979	0.9620	0.7549
Dys,Fat2ΔICD-Dys	0.9995	0.7944	1.0000	0.9986